Reaction forces on a relativistic point charge moving above a dielectric or a metallic half-space

D. Schieber and L. Schächter
Department of Electrical Engineering, Technion–Israel Institute of Technology, Haifa 32000, Israel
(Received 28 July 1997; revised manuscript received 15 December 1997)

We investigate the forces that act on a particle as it moves at a height h above a half-space of dielectric or lossy material. The expressions for the longitudinal and transverse forces are calculated numerically and analytic expressions are presented for limit cases. In a *dielectric* it is shown that the longitudinal force is zero at velocities below the Cherenkov velocity and it reaches a constant value at high energies. The transverse force below the Cherenkov velocity is the result of a superposition of evanescent waves only; in this regime it increases with the momentum. Above the Cherenkov velocity propagating waves add their contribution to the transverse force. For relatively low energies their contribution tends to increase the total force. At high energies the total transverse force decays as $1/\gamma$. In the case of a *metallic* medium (σ), the longitudinal force is proportional to $\sqrt{(\gamma\beta)^3/\sigma\eta_0 h}$ when this quantity is smaller than unity and it reaches a constant value when this parameter is much larger than unity. The transverse attraction force decreases monotonically with the relativistic factor γ. [S1063-651X(98)04205-6]

PACS number(s): 41.75.−i, 41.60.−m, 41.20.−q

INTRODUCTION

It is well known that if a charged particle moves in the vicinity of a dielectric at a velocity higher than the phase velocity of a plane wave in the corresponding material, then Cherenkov radiation is emitted; its spectrum is a topic that appears in many textbooks; see, e.g., [1]. This radiation comes at the expense of the kinetic energy of the particle. In a previous study [2] we calculated the deceleration force that acts on a particle as it moves in a *cylindrical* vacuum channel bored in an otherwise infinite dielectric material. In a similar way we calculated [2] the force that acts on the charge when the dielectric medium was replaced by a metal [3]. In all these cases the reaction force decelerates the particle. It was also shown [4,5] that the force becomes accelerating if the medium is active.

The motion of electrons above dielectric or metallic surfaces is of interest since this may become one of the attracting ways to generate millimeter and submillimeter wave radiation without excitation of multiple modes in the system. In particular, it is important to estimate the decelerating *longitudinal* force that acts on the moving particle due to its proximity to material, as well as the attracting force in the *transverse* direction. The advantages of open structures can be utilized in the case of particle accelerators, e.g., those which rely on the Smith-Purcell effect [6–10] or planar (quasiopen) structures manufacture using very-large-scale integrated technology, which recently has been attracting attention.

An extensive amount of work has been dedicated in the past to the motion of charged particles in the vicinity of a metallic half-space [11–18]. The main goal of these studies is electron spectroscopy; in other words, electrons scattered by a solid-state surface may provide important information about the characteristics of the medium. Specifically, excitation of plasmons and/or phonons [12,15,16,18] by grazing electrons has been investigated extensively. The assumptions common to all these studies is that the particles are *not relativistic* and for an effective ''interaction'' their distance from the surface is of the order of nanometers. The system envisioned in this study consists of relativistic (even ultrarelativistic) particles and their height above the surface is not smaller than a few micrometers. The goal of this study is to investigate the longitudinal and transverse forces on a bunch of charged particles as it moves above a metallic or dielectric half-space.

DEFINITION OF THE MODEL

Consider a charge $-q$ moving at a velocity v parallel to a half space of dielectric material ϵ_r. A Cartesian coordinate system is introduced: Its x coordinate is parallel to the motion of the particle and its y coordinate is transverse to the direction our particle moves, but parallel to the plane of interface between the dielectric ($z<0$) and the vacuum ($z>0$) as illustrated in Fig. 1. The electromagnetic field generated by this moving charge, as measured in the laboratory frame of reference in the absence of the dielectric half-space can be derived from the x component of the magnetic vector potential [$A_x^{(p)}=\beta\Phi^{(p)}$] and the scalar electric potential, which reads

$$\Phi^{(p)}=\frac{-q\gamma}{4\pi\epsilon_0}\frac{1}{2\pi}\int_{-\infty}^{\infty}dk_x dk_y e^{-j[k_x\gamma(x-vt)+k_y y]-|z-h|\sqrt{k_x^2+k_y^2}} \times\frac{1}{\sqrt{k_x^2+k_y^2}}. \tag{1}$$

The presence of the dielectric half-space causes additional (secondary) potentials in the upper region (superscripts s and u), which are given by

$$\begin{pmatrix} A_x^{(s,u)} \\ A_y^{(s,u)} \\ \Phi^{(s,u)} \end{pmatrix}=\frac{-q\gamma}{4\pi\epsilon_0}\frac{1}{2\pi}\int_{-\infty}^{\infty}dk_x dk_y \times\begin{pmatrix} \frac{v}{c^2}R_x \\ \frac{v}{c^2}R_y \\ R_x+\frac{k_y}{\gamma k_x}R_y \end{pmatrix} e^{-j[k_x\gamma(x-vt)+k_y y]-\sqrt{k_x^2+k_y^2}z}. \tag{2}$$

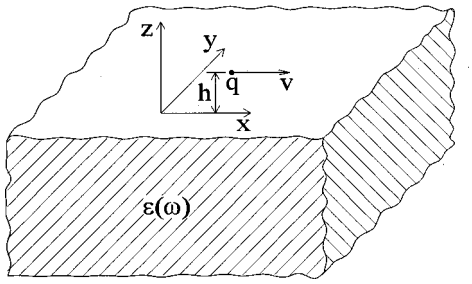

FIG. 1. Schematic of the system under consideration.

In expression (2) we used the Lorentz gauge. Similarly, the secondary potentials in the lower half-space (superscripts s,l) are given by

$$\begin{pmatrix} A_x^{(s,l)} \\ A_y^{(s,l)} \\ \Phi^{(s,l)} \end{pmatrix} = \frac{-q\gamma}{4\pi\epsilon_0}\frac{1}{2\pi}\int_{-\infty}^{\infty} dk_x dk_y \times \begin{pmatrix} \frac{v}{c^2}T_x \\ \frac{v}{c^2}T_y \\ \frac{1}{\epsilon_r}T_x + \frac{k_y}{\epsilon_r\gamma k_x}T_y \end{pmatrix} e^{-j[k_x\gamma(x-vt)+k_y y]+\Lambda z}, \tag{3}$$

where $\Lambda \equiv \sqrt{k_y^2+(\gamma k_x)^2(1-\epsilon_r\beta^2)}$. It should be pointed out that if the argument of the square root is negative, then there are two possibilities

$$\Lambda \equiv \begin{cases} +j\sqrt{|k_y^2+(\gamma k_x)^2(1-\epsilon_r\beta^2)|} & \text{for } k_x>0 \\ -j\sqrt{|k_y^2+(\gamma k_x)^2(1-\epsilon_r\beta^2|} & \text{for } k_x<0; \end{cases} \tag{4}$$

this is a direct result of the radiation condition.

In order to determine the amplitudes R_x, R_y, T_x, and T_y we impose the boundary conditions for the tangential field components (E_x, E_y, H_x, and H_y) at $z=0$. These provide us with four equations for the four amplitudes, i.e.,

$$\frac{k_x}{\gamma}(R_0+R_x)+k_y R_y = \frac{k_y}{\epsilon_r}T_y + k_x\gamma\left(\frac{1}{\epsilon_r}-\beta^2\right)T_x,$$

$$k_y(R_0+R_x)+\frac{k_y^2-\gamma^2\beta^2k_x^2}{\gamma k_x}R_y = \frac{k_y}{\epsilon_r}T_x + \frac{k_y^2-\gamma^2\beta^2\epsilon_r k_x^2}{\epsilon_r\gamma k_x}T_y, \tag{5}$$

$$-\sqrt{k_x^2+k_y^2}\,R_y = \Lambda T_y,$$

$$\sqrt{k_x^2+k_y^2}(R_0-R_x) = \Lambda T_x,$$

where

$$R_0(k_x,k_y) = \frac{e^{-\sqrt{k_x^2+k_y^2}h}}{\sqrt{k_x^2+k_y^2}}. \tag{6}$$

Since we are interested only in the force that acts on the particle, we present here the explicit solution in the upper space, i.e., the amplitudes R_x and R_y. For this purpose, we substitute T_x and T_y and obtain

$$R_x = -\frac{\epsilon_r-1}{\epsilon_r}\frac{k_x^2(\Lambda+\gamma^2 k)+k_y^2(\Lambda-k)}{k(\Lambda+k)(k+\Lambda/\epsilon_r)}R_0,$$

$$R_y = -\frac{\epsilon_r-1}{\epsilon_r}\frac{2\gamma k_x k_y}{(\Lambda+k)(k+\Lambda/\epsilon_r)}R_0. \tag{7}$$

With these expressions the forces that act on the particle ($x=vt$, $y=0$, $z=h$) read

$$\begin{pmatrix} F_x \\ F_y \\ F_z \end{pmatrix} = \frac{q^2}{4\pi\epsilon_0}\frac{1}{2\pi}\int_{-\infty}^{\infty} dk_x dk_y R(k_x,k_y) \begin{pmatrix} jk_x \\ jk_y \\ \gamma \\ \frac{k}{\gamma} \end{pmatrix} e^{-kh}, \tag{8}$$

where $k \equiv \sqrt{k_x^2+k_y^2}$ and $R(k_x,k_y) \equiv R_x(k_x,k_y)+(\gamma k_y/k_x)R_y(k_x,k_y)$, which after substituting the two expressions (7) reads

$$R = -\frac{\epsilon_r-1}{\epsilon_r}\frac{\Lambda k+\gamma^2(k^2+\beta^2k_y^2)}{(\Lambda+k)(k+\Lambda/\epsilon_r)}R_0. \tag{9}$$

Next we examine the three expressions (8) for two different cases: (i) lossless dielectric (Cherenkov) and (ii) lossy material (Ohm).

FORCES EXPERIENCED ABOVE A DIELECTRIC MEDIUM

In the case of a material characterized by a scalar dielectric material it is convenient to use instead the ''Cartesian'' integration variables k_x and k_y, a cylindrical set such that

$$k_x = k\cos\psi, \quad k_y = k\sin\psi. \tag{10}$$

In addition, we define

$$f(\psi,\gamma) \equiv \sin^2\psi + \gamma^2(1-\epsilon_r\beta^2)\cos^2\psi \tag{11}$$

and bearing in mind that all the force components are real functions [see Eq. (4)] we can write for the amplitude in Eq. (9) the expression

$$\overline{R}(\psi,\gamma) \equiv -\frac{\epsilon_r-1}{\epsilon_r}\frac{\xi+\gamma^2+\gamma^2\beta^2\sin^2\psi}{(1+\xi)(1+\xi/\epsilon_r)}, \tag{12}$$

$$\xi(\psi,\gamma) \equiv \sqrt{|f(\psi,\gamma)|}\begin{cases} +1 & \text{for } f(\psi,\gamma)>0 \\ +j & \text{for } f(\psi,\gamma)<0. \end{cases}$$

With these definitions the three components of the force that acts on the particle read

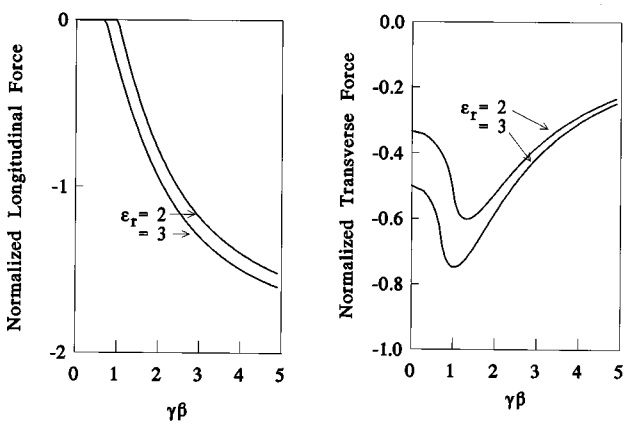

FIG. 2. Normalized forces acting on a charged particle as it moves above a dielectric half-space. The left frame illustrates the longitudinal force and the right frame the transverse force. The normalized longitudinal force has an asymptotic value of 2. The transverse force peaks in the vicinity of the Cherenkov condition, i.e., $\beta \sim 1/\sqrt{\epsilon_r}$. The normalization is with respect to $q^2/4\pi\epsilon_0(2h)^2$.

$$\begin{pmatrix} F_x(\gamma) \\ F_y(\gamma) \\ F_z(\gamma) \end{pmatrix} = \frac{q^2}{4\pi\epsilon_0(2h)^2}\frac{1}{2\pi}\int_{-\pi}^{\pi} d\psi\, \overline{R}(\psi,\gamma) \begin{pmatrix} j\cos\psi \\ \frac{j}{\gamma}\sin\psi \\ \frac{1}{\gamma} \end{pmatrix}. \tag{13}$$

Note that in these expressions k does not appear explicitly. This is because the integration over k is simple and is given by

$$\int_0^{\infty} dk\, k\, e^{-2kh} = \frac{1}{(2h)^2}. \tag{14}$$

Furthermore, since $\overline{R}$ is an even functions of ψ [see Eq. (12)], it is evident that the integrand of F_y is an odd function of ψ and as such, the integral of F_y vanishes, as expected due to the left-right symmetry of the system.

The other two components (longitudinal and transverse) of the force have been calculated numerically. The general case is illustrated in the two frames of Fig. 2 for $\epsilon_r = 2$ and 3. As expected, the decelerating force is nonzero if the velocity particle is above the Cherenkov condition ($\beta > 1/\sqrt{\epsilon_r}$) and it approaches the asymptotic value of

$$F_x(\gamma \gg 1) \simeq -\frac{q^2}{4\pi\epsilon_0(2h)^2} \times 2, \tag{15}$$

at high energies. This result is similar to the case when the particle moves in a dielectric channel of radius R:

$$F_x(\gamma \gg 1) \simeq -\frac{q^2}{4\pi\epsilon_0 R^2} \times 2. \tag{16}$$

It is interesting to note that the factor 2 occurs in both cases. However, if the particle is at the same distance from the dielectric, i.e., $h = R$, then the force is 4 times smaller in the planar case.

Expression (15) can be proved analytically. With this purpose in mind, we observe that if $\gamma \to \infty$ then the main contribution to the integral for F_x is from the region around $\psi \simeq \pm \pi/2$. It is convenient now to define $\psi = \pi/2 - \delta$, where $|\delta| \ll \pi/2$ and it represents one out of the four main contributions. With this definition it is possible to approximate ξ with

$$\xi(\delta,\gamma) \simeq j\gamma\delta\sqrt{\epsilon_r - 1}. \tag{17}$$

When evaluating the longitudinal force we have to take into consideration all four (identical) contributions; hence the resulting integral reads

$$F_x(\gamma \gg 1) \simeq -\frac{q^2}{4\pi\epsilon_0(2h)^2} \times \frac{4}{2\pi}\frac{1}{\epsilon_r} \mathrm{Re}\left\{ j\int_0^{\delta_0} d(-\delta) \times \frac{2\gamma^2\delta(\epsilon_r - 1)}{(1 + j\gamma\delta\sqrt{\epsilon_r - 1})(1 + j\gamma\delta\sqrt{\epsilon_r - 1}/\epsilon_r)} \right\}. \tag{18}$$

Upon defining a new variable $u = \gamma\delta\sqrt{\epsilon_r - 1}$ and denoting the new limits of integration by $(0, u_0)$, the integral can be calculated analytically:

$$F_x(\gamma \gg 1) \simeq -\frac{q^2}{4\pi\epsilon_0(2h)^2}\frac{4}{\pi}\frac{1}{\epsilon_r - 1} \times \left[\int_0^{u_0} du\, \frac{1}{1 + (u/\epsilon_r)^2} - \int_0^{u_0} du\, \frac{1}{1 + u^2} \right]. \tag{19}$$

If we assume that $u_0 \equiv \delta_0\gamma\sqrt{\epsilon_r - 1}$ is much larger than unity, we obtain exactly the result in Eq. (15).

The *transverse* force (F_z) presented in Fig. 2 will be referred to as the image-charge force since when the particle is at rest, the force corresponds to that of an image charge located at a distance $2h$ from the original one, inside the dielectric medium, its charge being $q(\epsilon_r - 1)/(\epsilon_r + 1)$. In order to understand the behavior of the image-charge force it will be convenient to examine more closely the integrand

$$\widetilde{R} \equiv \widetilde{R}/\gamma \tag{20}$$

of the integral corresponding to F_z. Figure 3 illustrates this integrand as a function of the variable ψ (for $\epsilon_r = 4$). It shows that as long as the particle's energy is below the Cherenkov condition, i.e., $\gamma \leqslant \gamma_c$ where $\gamma_c \equiv [1 - \beta_c^2]^{-1/2}$ and $\beta_c \equiv 1/\sqrt{\epsilon_r}$, the integrand is a monotonic function of ψ. Its absolute value increases with γ. Consequently, the force that acts on this particle increases monotonically. When the energy of the particle exceeds γ_c, i.e., above the Cherenkov condition, the integrand $\widetilde{R}$ has a minimum value at the point where $f(\psi,\gamma) = 0$, which defines the so-called Cherenkov angle

$$\psi_c(\gamma,\epsilon_r) \equiv \arctan(\gamma\sqrt{\epsilon_r\beta^2 - 1}). \tag{21}$$

This angle splits the integration region into two parts: (a) the contribution of the regular *evanescent* waves, which is between $\psi_c(\gamma,\epsilon_r)$ and $\pi/2$, and (b) the contribution associated

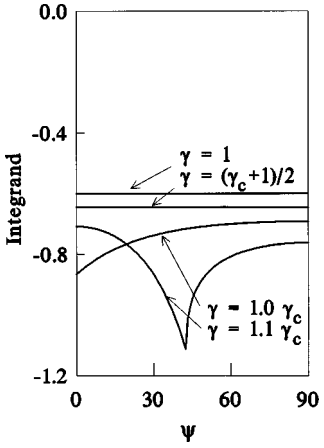

FIG. 3. Integrand $\widetilde{R}$ of the integral for the transverse force as a function of ψ. Below the Cherenkov condition ($\gamma \leqslant \gamma_c$) it is a monotonic function of ψ and its absolute value increases with γ. For $\gamma > \gamma_c$ the integrand has a peak determined by $f(\psi,\gamma)=0$.

with the propagating waves between 0 and $\psi_c(\gamma,\epsilon_r)$; we shall refer to this contribution as the Cherenkov image-charge force since it vanishes for $\gamma < \gamma_c$; note that these waves occur only in the dielectric half-space. Before we examine these two contributions let us examine the variation of three limiting cases of the integrand $\widetilde{R}(\psi=0,\gamma)$, $\widetilde{R}(\psi=\psi_c(\gamma),\gamma)$, and $\widetilde{R}(\psi=\pi/2,\gamma)$ as a function of γ. The left frame in Fig. 4 shows that the last two terms are linear with γ (for $\gamma > \gamma_c$) and always negative. This is not the case when $\psi=0$ and based on this specific case we conclude that there is an entire range of angles ψ for which the contribution of the propagating waves is positive. In other words, part of the Cherenkov radiation emitted in the dielectric tends to *repel* the point charge. In quantum-mechanical terms, the ''Cherenkov photon'' emitted in the dielectric medium has some momentum in the transverse (z) direction and at certain angles (and energies) this momentum is balanced by the particle, otherwise the medium serves as a ''momentum reservoir.'' For any given angle there is a critical energy $\gamma_{\rm cr}$,

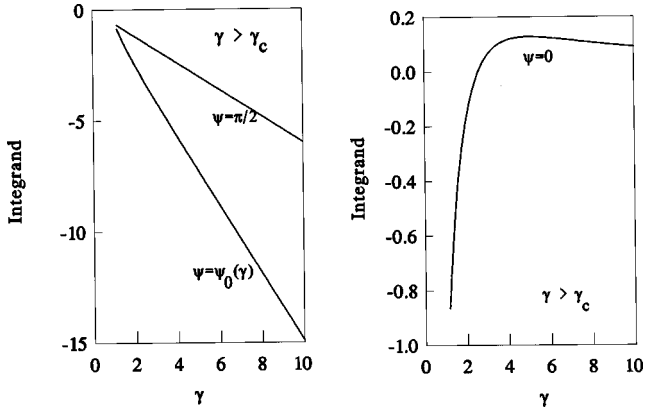

FIG. 4. Integrand $\widetilde{R}$ of the integral for the transverse force. The left frame illustrates $\widetilde{R}(\psi=\psi_c(\gamma),\gamma)$ and $\widetilde{R}(\psi=\pi/2,\gamma)$ as a function of γ; both functions are monotonic and negative. On the right we plot $\widetilde{R}(\psi=0,\gamma)$ and as clearly revealed, this quantity can become positive corresponding to a repelling contribution to the transverse force.

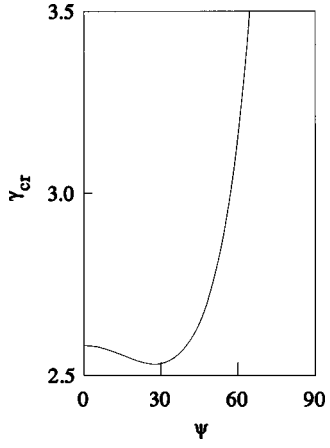

FIG. 5. Variation of the critical energy ($\gamma_{\rm cr}$) as a function of the angle ψ. For energies larger than ($\gamma_{\rm cr}$) the contribution of the integrand is positive, see the right frame of Fig. 4.

defined as $\mathrm{Re}[\widetilde{R}(\psi,\gamma_{\rm cr})]=0$, beyond which the contribution to the force is positive. Figure 5 shows the variation of this critical energy as a function of ψ (for $\epsilon_r=4$).

At this point we are in a good position to explain the behavior of the image-charge force. For this purpose we define the Cherenkov contribution to this force as

$$F_z^{\{C\}}(\gamma) \equiv \frac{q^2}{4\pi\epsilon_0(2h)^2}\left[\frac{2}{\pi}\int_0^{\psi_c(\gamma)} d\psi\, \widetilde{R}(\psi,\gamma)\right] \quad (22)$$

and we shall refer to the ''regular'' contribution as the evanescent contribution defined as

$$\overline{F_z^{\{E\}}}(\gamma) \equiv \frac{q^2}{4\pi\epsilon_0(2h)^2}\left[\frac{2}{\pi}\int_{\psi_c(\gamma)}^{\pi/2} d\psi\, \widetilde{R}(\psi,\gamma)\right]. \quad (23)$$

The two contributions are plotted in Fig. 6, which reveals

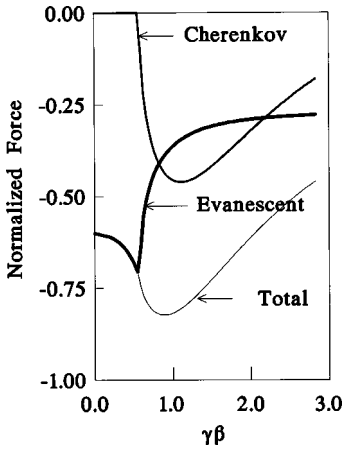

FIG. 6. Two contributions to the transverse force as a function of the momentum of the particle. Below the Cherenkov condition only the evanescent waves contribute and the net force increases with the momentum ($\gamma\beta$). Above the Cherenkov condition the evanescent wave contribution decreases to an asymptotic value that depends only on the dielectric coefficient. The Cherenkov contribution increases up to a maximum value, beyond which the repelling contribution starts to be significant and it reduces this force. The normalization is with respect to $q^2/4\pi\epsilon_0(2h)^2$.

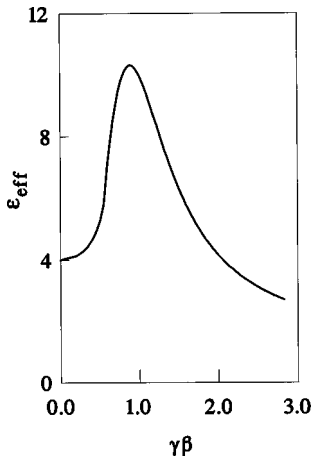

FIG. 7. Effective dielectric coefficient as ''measured'' by the moving particles as a function of its momentum.

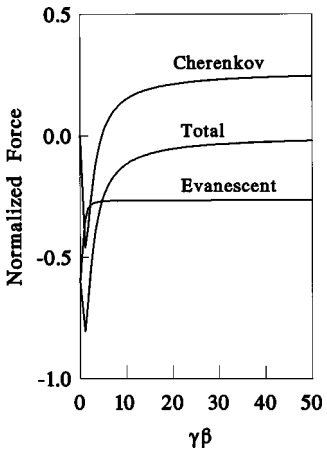

FIG. 8. Two contributions to the transverse force (Cherenkov and evanescent) as a function of the momentum. The evanescent waves contribution is always negative, whereas the Cherenkov part changes sign and becomes repelling. The total force is always negative. The normalization is with respect to $q^2/4\pi\epsilon_0(2h)^2$.

several interesting trends. (i) Below the Cherenkov condition only the evanescent waves contribute and the net force increases with the momentum ($\gamma\beta$). As will be shown subsequently, this is equivalent to a situation in which the moving charge experiences a force that corresponds to a larger dielectric coefficient or, equivalently, the polarization field ''measured'' by a moving charge is larger than that experienced by a stationary one. (ii) Above the Cherenkov condition the evanescent wave contribution decreases to an asymptotic value that depends entirely on the dielectric coefficient. This asymptotic behavior can be understood if we recall that the integrand increases linearly with γ (see Fig. 4) and at the same time the integration interval is inversely proportional to γ. (iii) Both the evanescent and the Cherenkov contributions are discontinuous (as a function of the momentum) at $\beta=\beta_{\rm cr}$. However, the two ''discontinuities'' cancel each other and the total force is continuous. (iv) The Cherenkov contribution increases up to a maximum value, beyond which the repelling contribution starts to be significant and it reduces this force. The two opposite trends in the behavior of the Cherenkov and evanescent contributions are responsible for the peak in the image charge force as revealed in the right frame in Fig. 2.

Before we proceed with the investigation of the Cherenkov force at the ultra-relativistic limit it is instructive to examine the result of the total force as plotted in Fig. 6 from the point of view of the moving charge. Let us assume that the latter is ''aware'' of the fact that it is located above a dielectric half-space, which means that the force it will experience can be interpreted in terms of an effective dielectric coefficient

$$F_z=-\frac{q^2}{4\pi\epsilon_0(2h)^2}\frac{\epsilon_{\rm eff}-1}{\epsilon_{\rm eff}+1}. \tag{24}$$

Figure 7 illustrates the effective dielectric coefficient this observer will experience as a function of its momentum (for $\epsilon_r=4$). When at rest it obviously experiences a dielectric coefficient of 4 and for relatively low energies it increases to a peak value (in this case ~ 10), after which it drops to values below 4. This infers that the polarization field measured by the particle varies substantially for the various velocities.

Let us examine now the image-charge force at the ultrarelativistic limit. The evanescent contribution is expected to have a constant value that has been calculated already. There are two interesting questions that can be addressed: Is it possible that the Cherenkov contribution will become positive (we observed the trend to approach zero in Fig. 6) and is it possible that the total image-charge force will become positive (i.e., repelling)? In order to answer these questions we have calculated numerically the integrals for larger values of γ and the result is presented in Fig. 8. As clearly revealed by the curves, the Cherenkov image-charge force does reverse its sign; however, its value is always smaller than the contribution of the evanescent waves. In fact, it can be shown that the *total* image-charge force is inversely proportional to γ.

This asymptotic behavior can be proved analytically and for this purpose we pursue a similar procedure as in the case of the longitudinal force. The result is

$$\begin{aligned} F_z(\gamma\gg 1) &\simeq \frac{q^2}{4\pi\epsilon_0(2h)^2\gamma}\frac{4}{2\pi}\mathrm{Re}\left\{\int_0^{\delta_0} d(-\delta)\right. \\ &\quad\left.\times\frac{2\gamma^2(\epsilon_r-1)/\epsilon_r}{(1+j\gamma\delta\sqrt{\epsilon_r-1})(1+j\gamma\delta\sqrt{\epsilon_r-1/\epsilon_r})}\right\} \\ &\simeq \frac{q^2}{4\pi\epsilon_0(2h)^2\gamma}\frac{4\gamma}{\pi\sqrt{\epsilon_r-1}} \\ &\quad\times\left[\arctan(u_0)-\arctan\left(\frac{u_0}{\epsilon_r}\right)\right] \\ &\simeq -\frac{q^2}{4\pi\epsilon_0(2h)^2}\frac{1}{\gamma}, \end{aligned} \tag{25}$$

where this time $u_0=\gamma(\pi/2)\sqrt{\epsilon_r-1}$ was taken at its extremum value and it was assumed that it is much larger than unity; this is validated by the fact that $\gamma\gg 1$. This asymptotic behavior of the transverse force has important implications since for high-energy particles it becomes much smaller than

for a motionless particle releasing the constraint on the transverse dynamics of the particle above a dielectric medium.

FORCES EXPERIENCED ABOVE A METALLIC MEDIUM

It has been suggested in the past that electrons can be accelerated by using the inverse of the Smith-Purcell effect. Briefly, the idea is that a laser beam illuminates a grating and it generates a broad spectrum of spatial harmonics. One of these harmonics may accelerate the particle. We shall not discuss here the interaction of the bunch with an external radiation field, but we shall utilize the formalism developed above in order to estimate the ''dc'' effect of a *smooth* metallic surface on the particle.

The starting point is to replace the dielectric half-space with a lossy medium characterized by a conductivity σ; hence

$$\epsilon_r = 1 - j\,\frac{\sigma}{k_x \gamma\beta c \epsilon_0}. \tag{26}$$

It is convenient to define

$$\bar{\sigma} \equiv \sigma \eta_0 h \tag{27}$$

and $u = kh$; $\eta_0 = \sqrt{\mu_0/\epsilon_0}$. Using this notation it can be shown that $\Lambda h = u\sqrt{1 + j\bar{\sigma}\gamma\beta\,\cos\psi/u}$ and the three components of the force in Eq. (8) are given by

$$\begin{pmatrix} F_x(\gamma\beta) \\ F_y(\gamma\beta) \\ F_z(\gamma\beta) \end{pmatrix} = \frac{-q^2}{4\pi\epsilon_0 h^2} \int_0^\infty du\; u\; e^{-2u}\, \frac{1}{2\pi} \int_{-\pi}^{\pi} d\psi \begin{pmatrix} j\,\cos\psi \\ \frac{j}{\gamma}\sin\psi \\ \frac{1}{\gamma} \end{pmatrix} \frac{1 + (\gamma\beta)^2\,\dfrac{1+\sin^2\psi}{1+\sqrt{1+j\bar{\sigma}\gamma\beta\,\cos\psi/u}\;\mathrm{sgn}(\psi)}}{1 + j\,\dfrac{\gamma\beta}{\bar{\sigma}}\,u\,\cos\psi\,[1+\sqrt{1+j\bar{\sigma}\gamma\beta\,\cos\psi/u}\;\mathrm{sgn}(\psi)]}, \tag{28}$$

where $\mathrm{sgn}(\psi) = 1.0$ if $\cos\psi > 0$ and -1 otherwise. These expressions are exact since no approximations have been employed so far. We shall next examine the *longitudinal* force. The quantity $\bar{\sigma}$ is much larger than 1 for all practical metals and h of interest. Furthermore, the quantity

$$\bar{\sigma}\gamma\beta|\cos\psi|\,\frac{1}{u} \gg 1 \tag{29}$$

can be considered to be much larger than unity since the contribution of the integrand to F_x when this condition is not satisfied ($\psi = \pm\pi/2$ or $u \to \infty$) is zero. Consequently,

$$F_x \simeq \frac{-q^2}{4\pi\epsilon_0 h^2} \int_0^\infty du\; u\; e^{-2u}\, \frac{1}{2\pi} \times \int_{-\pi}^{\pi} d\psi\,\cos\psi\,(j)\, \frac{1 + \dfrac{1+\sin^2\psi}{\sqrt{j\alpha\,\cos\psi/u}\;\mathrm{sgn}(\psi)}}{1 + j\sqrt{\dfrac{j}{\alpha}\cos\psi u}\;\mathrm{sgn}(\psi)\cos\psi}, \tag{30}$$

where we used

$$\alpha \equiv \bar{\sigma}/(\gamma\beta)^3. \tag{31}$$

It is important to emphasize that in contrast to the parameter $\bar{\sigma}$, which for all practical metals is much larger than unity (even if h is of order of a few micrometers), the parameter α can be either smaller or larger than 1 according to the momentum of the point charge. The variation of the longitudinal force with γ is illustrated in Fig. 9. For the range of parameters presented in Fig. 9, there is virtually no difference between the values calculated using the exact expression (28) and the approximation (30).

One case can be evaluated analytically and it corresponds to the limit when $\alpha \gg 1$ or $\bar{\sigma} \gg (\gamma\beta)^3$. For this purpose the integrand can be approximated by

$$\frac{1 + \dfrac{1+\sin^2\psi}{\sqrt{j\alpha\,\cos\psi/u}\;\mathrm{sgn}(\psi)}}{1 + j\sqrt{\dfrac{j}{\alpha}u\,\cos\psi}\;\mathrm{sgn}(\psi)\cos\psi} \simeq 1 + \frac{1+\sin^2\psi}{\sqrt{j\alpha\,\cos\psi/u}\;\mathrm{sgn}(\psi)} - j\sqrt{\frac{j}{\alpha}\cos\psi u} \times \mathrm{sgn}(\psi)\cos\psi \tag{32}$$

and since the first term does not contribute to the integral, the force is given by

$$\frac{F_x}{-q^2/4\pi\epsilon_0 h^2\sqrt{\alpha}} = \left(\int_0^\infty u^{1.5} e^{-2u}\right) \times \left(\frac{1}{2\pi}\,\frac{\sqrt{2}}{2}\,4\int_0^{\pi/2} d\psi\,(1+\sin^2\psi)\sqrt{\cos\psi}\right) + \left(\int_0^\infty u^{1.5} e^{-2u}\right) \times \left(\frac{1}{2\pi}\,\frac{\sqrt{2}}{2}\,4\int_0^{\pi/2} d\psi\,\cos^{2.5}\psi\right). \tag{33}$$

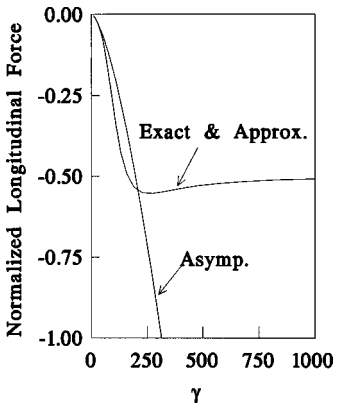

FIG. 9. Normalized longitudinal force acting on a charged particle as it moves above a metallic half-space; $\bar{\sigma}=2\times10^6$. The two solid lines represent the normalized force as determined from the exact expression (28) and the approximate expression (30). The two are identical for all practical purposes. The dashed line represents the asymptotic expression in Eq. (30). Note that it is a reasonable approximation up to $(\gamma\beta)^3\sim\bar{\sigma}$.

All the integrals can be evaluated numerically:

$$\int_0^\infty u^{1.5}e^{-2u}=0.235,$$

$$\frac{2}{\pi}\int_0^{\pi/2}d\psi(1+\sin^2\psi)\sqrt{\cos\psi}=1.068, \tag{34}$$

$$\frac{2}{\pi}\int_0^{\pi/2}d\psi\sqrt{\cos^5\psi}=0.458$$

and the result is

$$F_x\simeq-0.254\times\frac{q^2}{4\pi\epsilon_0h^2}\sqrt{\frac{(\gamma\beta)^3}{\sigma\eta_0h}}. \tag{35}$$

The asymptotic line in Fig. 9 represents this expression. We observe that it is a reasonable approximation up to $(\gamma\beta)^3\sim\bar{\sigma}$; in this calculation $\bar{\sigma}=2\times10^6$.

The result (35) should be compared with the decelerating force that acts on the same particle as it moves in a channel of radius R bored in the metallic medium; this is given by [2]

$$F_x\simeq-0.54\times\frac{q^2}{4\pi\epsilon_0R^2}\sqrt{\frac{(\gamma\beta)^3}{\sigma\eta_0R}}. \tag{36}$$

For $h=R$ and the same material and momentum, the force in the bored channel is slightly larger. This result can be understood in terms of the ''limited amount'' of material in the vicinity of the particle in the planar case compared to that in the cylindrical one.

As in the case of the dielectric medium, the y component of the force is zero due to the $\sin\psi$ function in the integrand; therefore, we shall next evaluate the transverse force, i.e., F_z. For a motionless particle $\beta=0$, it can be readily checked that the force corresponds exactly to that of an image charge and it is given by

$$F_z(\beta=0)=\frac{-q^2}{4\pi\epsilon_0(2h)^2}. \tag{37}$$

At high energies we pursue the same approach as previously [see the assumption (24); however, note that in this case the integrand no longer possesses the $\cos\psi$ term and therefore the contribution of the region close to $\pm\pi/2$ is nonzero]. Hence

$$F_z=-\frac{q^2}{4\pi\epsilon_0h^2}\int_0^\infty du\ u\ e^{-2u}\frac{1}{\gamma}\frac{4}{2\pi}\int_0^{\pi/2}d\psi \times\mathrm{Re}\left\{\frac{1+\dfrac{1+\sin^2\psi}{\sqrt{j\alpha\cos\psi/u}}}{1+j\sqrt{\dfrac{j}{\alpha}\cos\psi u\cos\psi}}\right\}, \tag{38}$$

which at the limit of $\alpha\gg1$ reads

$$F_z[\bar{\sigma}\gg(\gamma\beta)^3]\simeq-\frac{q^2}{4\pi\epsilon_0(2h)^2}\frac{1}{\gamma}. \tag{39}$$

Thus the attracting image-charge force is inversely proportional to the energy of the point charge as in the ultrarelativistic particle above a dielectric half-space.

TABLE I. Comparison of the reaction forces in planar and cylindrical geometries.

Geometry	Dielectric	Metal
planar	$F_\parallel(\gamma\gg1)\simeq-2\times\frac{q^2}{4\pi\epsilon_0(2h)^2}$	$F_\parallel(\sigma\eta_0h\gg\gamma^3\beta^3)\simeq-0.254\times\frac{q^2}{4\pi e_0h^2}\sqrt{\frac{(\gamma\beta)^3}{\sigma\eta_0h}}$
	$F_\perp(\gamma\gg1)\simeq-\frac{q^2}{4\pi\epsilon_0(2h)^2}\frac{8}{\pi^2}\frac{1}{\gamma}$	$F_\perp(\sigma\eta_0h\gg\gamma^3\beta^3)\simeq-\frac{q^2}{4\pi\epsilon_0(2h)^2}\frac{1}{\gamma}$
cylindrical	$F_\parallel(\gamma\gg1)\simeq-2\times\frac{q^2}{4\pi\epsilon_0R^2}$	$F_\parallel(\sigma\eta_0R\gg\gamma^3\beta^3)\simeq-0.54\times\frac{q^2}{4\pi\epsilon_0R^2}\sqrt{\frac{(\gamma\beta)^3}{\sigma\eta_0R}}$
		$F_\parallel(\gamma\gg1)\simeq-2\times\frac{q^2}{4\pi\epsilon_0R^2}$

DISCUSSION

We have investigated the reaction field that acts on a point charge as it moves above dielectric or metallic half-spaces. The longitudinal deceleration force is comparable to the case when a similar particle moves in a cylindrical channel bored in the same material. As in the latter case [2], the deceleration force in a dielectric medium has an asymptotic value that is *independent* of the energy and material.

The transverse (image-charge) force was also evaluated. In the dielectric case, at low energies, it was found to be larger than the force corresponding to the (motionless) image charge. After it reaches a peak value in the vicinity of the Cherenkov velocity, it decreases as $1/\gamma$. This reduced force can be explained in terms of the finite transverse momentum of the Cherenkov photon, which is balanced in part by the particle. In the case of a lossy material this force decreases monotonically with γ. This behavior suggests that the transverse attraction of an electron bunch in an open-structure accelerator might be less severe than previously thought. All the results are summarized in Table I and for convenience we also present the results from the case when the particle moves in a cylindrical channel bored in the same material.

ACKNOWLEDGMENTS

This study was supported by the United States Department of Energy, by the United States–Israel Bi-National Science Foundation, and by the Guthwirth Foundation.

[1] D. Jackson, *Classical Electrodynamics*, 2nd ed. (Wiley, New York, 1975), p. 638.
[2] L. Schächter and D. Schieber, Nucl. Instrum. Methods Phys. Res. A **388**, 8 (1997).
[3] A similar analysis has been performed by De Zutter *et al.* [J. Appl. Phys. **59**, 4146 (1986)], but their conclusions for ultrarelativistic particles are not accurate.
[4] L. Schächter, Phys. Lett. A **205**, 355 (1995).
[5] L. Schächter, Phys. Rev. E **53**, 6427 (1996).
[6] S. J. Smith and E. M. Purcell, Phys. Rev. **92**, 1069 (1953).
[7] R. B. Palmer, in *Laser Acceleration of Particles*, edited by P. J. Channel, AIP Conf. Proc. No. 91 (AIP, New York, 1982), p. 179.
[8] R. B. Palmer, N. Baggett, J. Claus, R. Fernow, I. Stumer, H. Figueroa, N. M. Kroll, W. Funk, G. Lee-Whiting, M. Pickup, P. Goldstone, K. Lee, P. Corkum, and T. Himel, in *Laser Acceleration of Particles*, edited by Chan Joshi and Thomas Katsouleas, AIP Conf. Proc. No. 130 (AIP, New York, 1985), p. 234.
[9] Kang-Je Kim and N. M. Kroll, in *Laser Acceleration of Particles* (Ref. [7]), p. 190.
[10] M. Pickup, in *Laser Acceleration of Particles* (Ref. [8]), p. 281.
[11] R. H. Ritchie, Phys. Rev. **106**, 874 (1957).
[12] N. Takimoto, Phys. Rev. **146**, 366 (1966).
[13] D. M. Newns, Phys. Rev. B **1**, 3304 (1970).
[14] R. Ray and G. D. Mahan, Phys. Lett. **42A**, 301 (1972).
[15] B. Gumhalter and D. M. Newns, Surf. Sci. **50**, 645 (1975).
[16] J. P. Muscat, Solid State Commun. **18**, 1089 (1976).
[17] J. P. Muscat and D. M. Newns, Surf. Sci. **64**, 641 (1977).
[18] A. Howie, Ultramicroscopy **11**, 141 (1983).